Talanta 94 (2012) 348–352

Contents lists available at SciVerse ScienceDirect

Talanta

journal homepage: www.elsevier.com/locate/talanta

Short communication

A new method for the identification and quantification of magnetite–maghemite mixture using conventional X-ray diffraction technique

Wonbaek Kim[a], Chang-Yul Suh[a], Sung-Wook Cho[a], Ki-Min Roh[a], Hanjung Kwon[a], Kyungsun Song[a,*], In-Jin Shon[b]

[a] Korea Institute of Geoscience & Mineral Resources (KIGAM), Gwahang-no 124, Yuseong-gu, Daejeon, 305- 350, Republic of Korea
[b] Division of Advanced Materials Engineering, Chonbuk National University, Chonbuk 561-756, Republic of Korea

ARTICLE INFO

Article history:
Received 20 January 2012
Received in revised form 2 March 2012
Accepted 2 March 2012
Available online 7 March 2012

Keywords:
Iron oxide
Magnetite
Maghemite
Wire explosion
X-ray diffraction
Deconvolution

ABSTRACT

The electrical explosion of Fe wire in air produced nanoparticles containing the binary mixture of magnetite (Fe_3O_4) and maghemite (γ-Fe_2O_3). The phase identification of magnetite and maghemite by the conventional X-ray diffraction method is not a simple matter because both have the same cubic structure and their lattice parameters are almost identical. Here, we propose a convenient method to assess the presence of magnetite–maghemite mixture and to further quantify its phase composition using the conventional peak deconvolution technique. A careful step scan around the high-angle peaks as (5 1 1) and (4 4 0) revealed the clear doublets indicative of the mixture phases. The quantitative analysis of the mixture phase was carried out by constructing a calibration curve using the pure magnetite and maghemite powders commercially available. The correlation coefficients, R^2, for magnetite–maghemite mixture was 0.9941. According to the method, the iron oxide nanoparticles prepared by the wire explosion in this study was calculated to contain 55.8 wt.% maghemite and 44.2 wt.% magnetite. We believe that the proposed method would be a convenient tool for the study of the magnetite–maghemite mixture which otherwise requires highly sophisticated equipments and techniques.

1. Introduction

X-ray diffraction technique has been an indispensable tool for the identification and characterization of various iron oxide phases. Nevertheless, the identification of magnetite ($Fe(II)Fe(III)_2O_4$) and maghemite (γ-$Fe(III)_2O_3$) phases by X-ray diffraction is quite intricate, because both phases possess the same spinel structure and almost identical lattice parameters.

In many previous studies, iron oxide particles have been successfully synthesized through various methods and indexed to maghemite or magnetite based on the fact that its lattice parameter was more close to one of the both phases [1–8]. Nevertheless, more researchers employed various supplementary analytical techniques in order to substantiate the identification of their iron oxides: wet chemical analysis [9–13], Mössbauer spectrometry [10,11,14–20], Raman spectroscopy [16,21,22], Fourier Transform Infrared (FT-IR) spectrophotometry [17,21,23–27], X-ray Photoelectron Spectroscopy (XPS) [16,28,29], Field Emission Transmission Microscopy with Selected Area Diffraction (FE-TEM/SAD) [4,16,18,27,30–36]. It appears that these techniques were very successful for this purpose especially when the sample was a single phase magnetite or maghemite.

Mössbauer spectrometry has been considered to be the most suitable technique, because the magnetite spectra consist of two discrete sextets [10,11,17–20]. Even though Mössbauer spectroscopy can provide most reliable quantitative data, it often suffers from the difficulties in fitting the complicated spectra [17,37]. Furthermore, the differentiation between non-stoichiometric magnetite and magnetite–maghemite mixture was claimed to be almost impossible [38,39]. The quantification of Fe(II) and Fe(III) has been widely attempted by the traditional wet-chemical method, though an extreme care should be practiced to prevent the oxidation of magnetite during the measurement routine [11]. XPS is a surface-sensitive analytical tool providing little information on the bulk properties. For example, the preferential oxidation on the surface of magnetite to maghemite was successfully analyzed using XPS [28,29]. A simple FT-IR has also been adopted for the quantification of iron-oxide mixture phase using a calibration curve with relatively low coefficient of determination of R^2 [25].

As stated above, numerous analytical techniques have been utilized to differentiate the magnetite and maghemite powders produced by various methods. Nevertheless, to the best knowledge of the authors, the quantitative analysis of magnetite–maghemite

* Corresponding author. Tel.: +82 42 868 3640; fax: +82 42 868 3393.
E-mail address: kssong@kigam.re.kr (K. Song).

0039-9140/$ – see front matter © 2012 Elsevier B.V. All rights reserved.
doi:10.1016/j.talanta.2012.03.001

Table 1
Iron oxide powders synthesized by the wire explosion in this study and the commercial powders used to prepare the standard mixture samples of known compositions.

Sample	Maker	Particle size	Lattice parameter (Å)
Iron oxide	This study	33.8 ± 20.6 nm	8.3763 ± 0.006
Magnetite (Fe_3O_4)	Sigma–Aldrich no.310069	1 μm	8.396 (JCPDS 19-629)
Maghemite (γ-Fe_2O_3)	Sigma–Aldrich no. 544884	<50 nm	8.3515 (JCPDS 39-1346)

mixture by the X-ray diffraction method has never been attempted. The iron oxide powders produced by the wire explosion in this study appeared to contain both phases. Therefore, in the course of the study on this subject, we could elaborate a simple way to verify the existence of the magnetite–maghemite mixture and to further quantify their relative compositions. For the quantification of the mixture, a calibration curve was constructed from the standard mixtures of known compositions using the commercial magnetite and maghemite powders.

2. Experimental procedure

2.1. Electrical explosion

The explosion device consists of a high voltage dc power supply, a bank of capacitors, a plasma switch and an explosion chamber. The plasma switch initiates the discharge. The capacitance of the exploding circuit was 3.5 μF and the applied voltage across the 20 mm-long wire was 11.4 kV. Therefore, the stored energy was about 227 J about 80–90% of which was considered to be transferred to the wire. The diameter of Fe wire for the explosion experiment was 0.3 mm. To begin with, the explosion chamber was evacuated and flushed with pure argon gas. The explosion experiment was conducted in a 30-l stainless chamber with the cover plate loosely tightened. The total number of explosions for each condition was about 600. After the explosion, the powders were filtered through a 125 μm sieve to remove some misfired portions. The morphology of the nanopowders were examined by FE-TEM (Field-Emission Transmission Electron Microscope, model JEM-2010F, JEOL Ltd., Japan).

2.2. X-ray diffraction

X-ray diffraction (XRD, D/MAX 2200, Rigaku Corp., Japan) study was conducted with Cu K_α radiation equipped with a graphite monochromator. A continuous scan XRD data were collected at diffraction angles between 20° and 80° operating at 40 mA and 40 kV. The step scan was conducted typically under the following conditions: 2θ range 56–58.5° for (5 1 1) peak and 61–64° for (4 4 0) peak; with the step width 0.01°; counting time of 10 s. The peak deconvolution and lattice parameter measurement were carried out using the MDI Jade 6.5 program furnished with the XRD. The data profiles were fit with a pseudo-Voigt profile function. TEM micrographs were analyzed for particle size measurement using a commercial image processing software (Image-Pro Plus 4.5.1). The particle size distribution was rather broad and the average particle size measured for more than 500 particles was 33.8 ± 20.6 nm.

2.3. Calibration curve

To quantify the binary mixture, the standard mixture samples were prepared by mixing the pure magnetite and maghemite powders commercially available. Table 1 shows the commercial powders used to make the mixture samples along with the powders synthesized in this study. The X-ray diffraction patterns from the magnetite and maghemite matched exactly to JCPDS 19-629 and JCPDS 39-1346, respectively. No other phases were observed. Six reference samples (0 wt.%, 20 wt.%, 40 wt.%, 60 wt.%, 80 wt.%, 100 wt.% maghemite) containing corresponding amounts of magnetite and maghemite powders were mixed as listed in Table 2. All step scan X-ray diffraction experiments were performed at least in triplicate, and the average values were used to construct the calibration curve.

Table 2
The standard mixture samples prepared by mixing the commercial maghemite and magnetite powders.

Samples	Composition
0%	Pure magnetite
20%	20 wt.% maghemite + 80 wt.% magnetite
40%	40 wt.% maghemite + 60 wt.% magnetite
60%	60 wt.% maghemite + 40 wt.% magnetite
80%	80 wt.% maghemite + 20 wt.% magnetite
100%	Pure maghemite

3. Results and discussion

3.1. X-ray diffraction study of the explosion products

Fig. 1 shows the X-ray diffraction pattern of nanoparticles synthesized by the wire explosion in this study. It shows a cubic structure which may be indexed to either magnetite or maghemite. No other peaks from other oxide phases as hematite or wüstite were noticed. As previously stated, the lattice parameters of the magnetite and maghemite phases are very close and difficult to be differentiated unless it is a single phase of well-crystallized structure. In this study, the lattice parameter calculated from the pattern in Fig. 1 was 8.3763 Å (see Table 1) which lies between that of magnetite and maghemite (8.396 Å and 8.3515 Å, see Table 1). Therefore, it was not possible for us to decide whether the reaction product is the magnetite or the maghemite. We supposed that it may be a mixture of both phases.

Supposedly, the maghemite phase is known to exhibit few extra peaks at 23.77° (2 1 0) and 26.10° (2 1 1) which may possibly be used to distinguish it from the magnetite phase. However, in reality, the intensities of these peaks are very weak (5%) for the positive

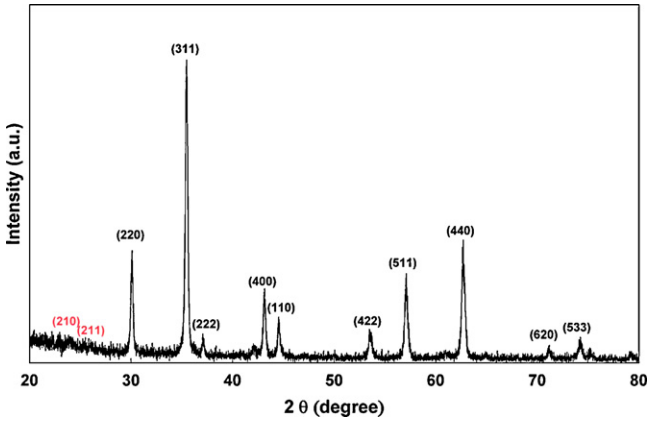

Fig. 1. X-ray diffraction pattern from the iron oxide nanoparticles produced by the explosion of Fe wire in air. Here, the peaks correspond to either magnetite or maghemite phase though the (2 1 0) and (2 1 1) peaks which are the characteristic peaks of the maghemite phase are not obvious.

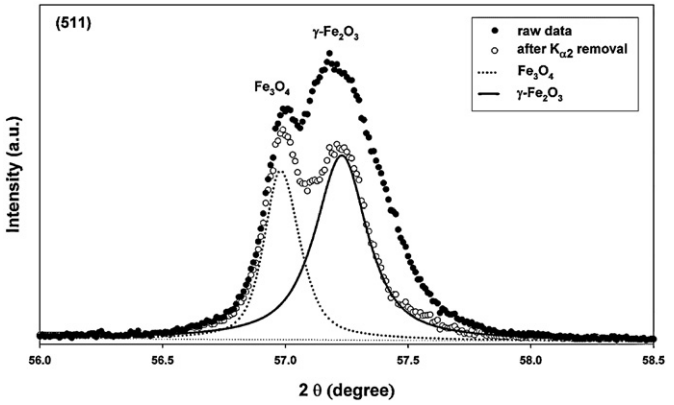

Fig. 2. A typical step scan pattern of (5 1 1) peak from nanoparticles produced by the explosion of Fe wire in air. The peak is deconvolutioned into the magnetite (Fe_3O_4) and maghemite (γ-Fe_2O_3). Here, ● represents the raw pattern and ○ represents the pattern after $K_{\alpha 2}$ removal.

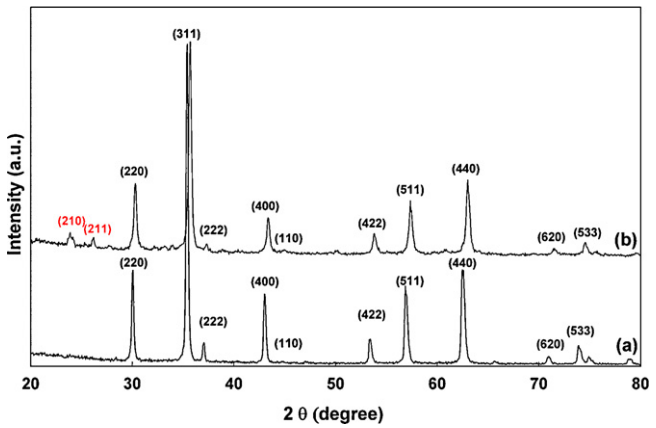

Fig. 3. X-ray diffraction patterns of the commercial powders used to prepare the standard mixture samples. The characteristic (2 1 0) and (2 1 1) peaks of the maghemite phase are obvious: (a) magnetite (Fe_3O_4), Sigma–Aldrich 310069 (b) maghemite (γ-Fe_2O_3), Sigma–Aldrich 544884.

identification of the maghemite phase. In addition, even though one can observe these extra peaks from the maghemite phase, it does not guarantee that it is a single phase maghemite since it could be a mixture of both phases.

Therefore, assuming that our iron oxide nanoparticles are a magnetite–maghemite mixture, we applied the step-scan method expecting to observe two peaks from both phases. Fig. 2 shows a typical step scan pattern of (5 1 1) peak taken at angles between 56° and 58.5°. Here, the peak profile delineated by ● shows the original data, which clearly shows two peaks at approximately 57° and 57.3°. The presence of both phases was more obvious after $K_{\alpha 2}$ was removed (delineated by ○). As a result, we assigned the 1st peak at lower angle as the magnetite peak and 2nd peak at higher angle as the maghemite peak. The peak deconvolution routine was carried out for $K_{\alpha 2}$-substracted peaks using JADE 6.5 program. Apparently, our postulation appears to be correct. Supposing that the iron oxide nanoparticles are the mixture of both magnetite and maghemite, it would be informative if we can determine the relative amount of each phase. We thus prepared the standard mixture samples using the commercial magnetite and maghemite powders to construct a calibration curve as will be explained in the following sections.

3.2. Preparation of standard magnetite–maghemite mixture

In the preparation of the standard mixture samples using the commercial powders (Table 1), it is very important to verify that each powder is not a mixture. This point is particularly important considering the recent report by Chowdhury et al. that the commercial magnetite they purchased for As removal study was not a single phase but a mixture of magnetite and maghemite [29]. Fig. 3 shows the X-ray diffraction patterns of both powders. They matched well with the standard patterns: magnetite with JCPDS 19-629 (Fig. 3a) and maghemite with JCPDS 39-1346 (Fig. 3b). However, according to our previous postulation, the close lattice parameter match would not be the enough condition for the verification of a single phase structure. Therefore, we applied the step scan routine to the commercial powders for the (5 1 1) and (4 0 0) peaks. The results showed that the peaks were quite symmetrical suggesting that both powders are not the mixture phases at least under our precision level (see 0% and 100% maghemite peaks in Fig. 4). It would also be helpful to note that the characteristic (2 1 0) and (2 1 1) peaks of the maghemite phase can be clearly observed in Fig. 3(b). Based on the previous results, we consider the commercial powders as the single-phase magnetite and maghemite from which a calibration curve can be constructed.

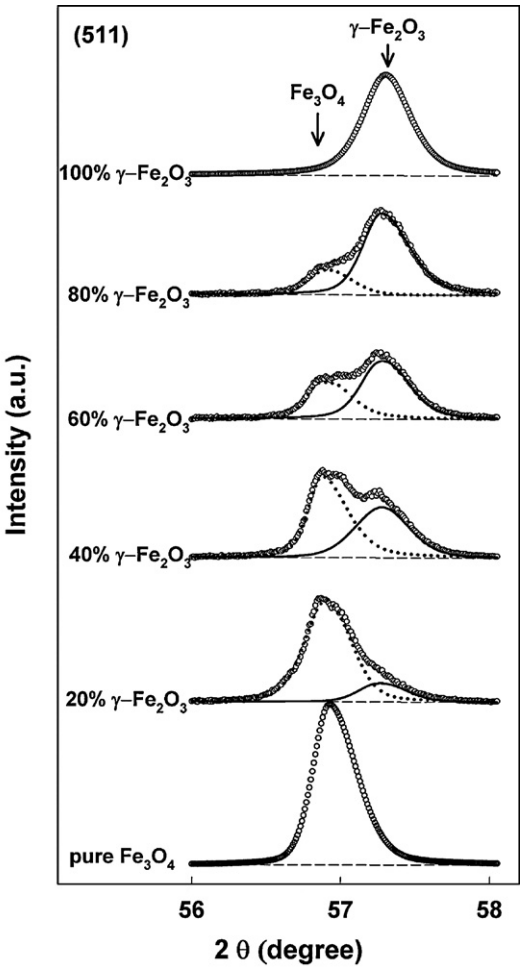

Fig. 4. Step scan X-ray diffraction patterns of (5 1 1) peak obtained from the standard samples of pre-determined compositions prepared by mixing the commercial magnetite (Fe_3O_4) and maghemite (γ-Fe_2O_3). Here, the lower angle peak represents the magnetite and the higher angle peak represents the maghemite phase.

3.3. Construction of the calibration curve

To construct a calibration curve for phase quantification, the standard mixture samples containing 0, 20, 40, 60, 80, and 100 wt.% maghemite were prepared (see Table 2). Fig. 4 shows the step scan

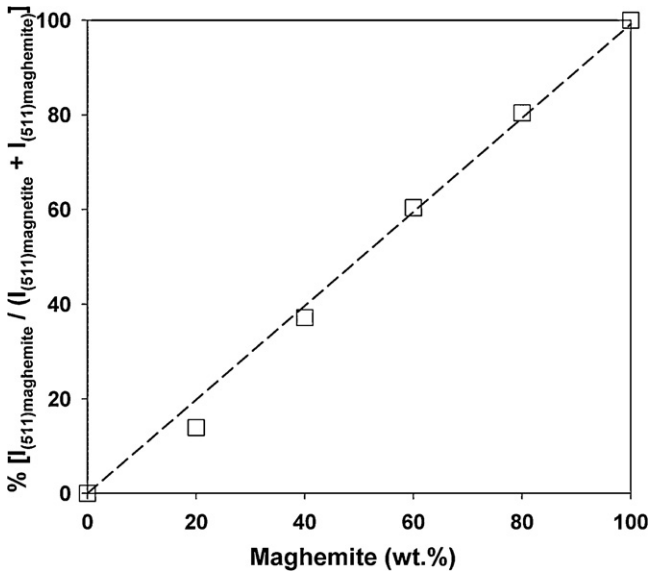

Fig. 5. A calibration curve showing the relationship between the pre-determined composition of magnetite–maghemite mixture (Table 2) and the measured integrated intensity % of maghemite phase.

results of (5 1 1) peaks from the six standard mixture samples. The peaks delineated by ○ are the patterns after $K_{\alpha 2}$ subtraction. Here, the magnetite (Fe_3O_4) and maghemite (γ-Fe_2O_3) peaks are marked by arrows on the figure. It is seen that the (5 1 1) peak was deconvolutioned into the magnetite and maghemite peaks in the same manner as shown previously in Fig. 2. The deconvolution of (4 4 0) peaks was also carried out and showed similar results (not shown).

The quantitative determination was based on the assumption that the amount of a phase is proportional to its integrated intensity fraction in the overlapping peak. For the magnetite–maghemite mixture, the amount of maghemite can be expressed from the integrated intensity fraction of the $(5\,1\,1)_{\text{maghemite}}$ peak as Eq. (1).

$$\left[\frac{I_{(5\,1\,1)\text{maghemite}}}{I_{(5\,1\,1)\text{maghemite}} + I_{(5\,1\,1)\text{maghemite})}}\right] = Kw_{\text{maghemite}} \quad (1)$$

where $I_{(5\,1\,1)\text{maghemite}}$ represents the deconvolutioned (5 1 1) peak intensity of the magnetite, $I_{(5\,1\,1)\text{magnetite}}$ the deconvolutioned intensity of the magnetite, $w_{\text{maghemite}}$ wt.% of the maghemite in the standard mixture, and K a constant. K can be determined from the calibration curve. Fig. 5 shows the relationship between the measured intensity % of maghemite $[I_{(5\,1\,1)\text{maghemite}}/(I_{(5\,1\,1)\text{magnetite}} + I_{(5\,1\,1)\text{maghemite}})]$ and wt.% of maghemite $[w_{\text{maghemite}}]$ for the standard mixture samples.

A linear relationship was found between the intensity fraction of maghemite and wt.% of maghemite in the standard mixture. The slope (K) was 1.0136 and y-intercept was −0.2371. The calibration curve is summarized as Eq. (2). Here, the coefficient of determination (R^2) was found to be 0.9941. The detection limit (DL) for the maghemite quantification in the mixture was estimated using the root mean square error (RMSE) method (Eq. (3)) [40]. RMSE describes the difference between predicted values and measured ones based on the linear calibration curve. The calculated detection limit for the maghemite was calculated to be 9.5 wt.% according to Eq. (3).

$$\left[\frac{I_{(5\,1\,1)\text{maghemite}}}{(I_{(5\,1\,1)\text{maghemite}} + I_{(5\,1\,1)\text{maghemite}}}\right] = 1.0136 \times w_{\text{maghemite}} - 0.2371 \quad (2)$$

$$\text{Detection Limit(DL)} = 3 \times \frac{\text{RMSE}}{\text{slope}} \quad (3)$$

3.4. Determination of phase composition of the wire explosion products

Now, following the method previously described above, we determined the phase composition of the nanoparticles prepared by the wire explosion technique in this study. When the suggested method was applied to our nanoparticles (see Fig. 2), the amount of maghemite and magnetite phases was calculated to be 55.8 wt.% and 44.2 wt.%, respectively. It is interesting that the amount of maghemite appears to be relatively high considering the fact that we could not positively locate the characteristic (2 1 0) and (2 1 1) peaks of the maghemite phase. On the contrary, the two characteristic peaks were clearly identified in the case of the commercial maghemite powder (see Fig. 3(a)). Considering this, it should be noted here that the absence or observation of the characteristic peaks may not be used as a sufficient criterion for the phase identification. As previously stated in the introduction, most of the previous studies report the synthesis of either a single-phase maghemite or magnetite. Therefore, it may be that the synthesis of magnetite–maghemite mixture phases in this study appears to indicate the inhomogeneous nature of the wire explosion reaction originating from the high energy deposition in a very short time. In any case, it should be worth mentioning that the step-scan routine as demonstrated in this study may provide a simple approach to identify and quantify other mixture phases whose lattice parameters do not allow an instant phase identification.

4. Conclusions

The electrical explosion of Fe wire in air produced iron oxide nanoparticles containing the mixture of magnetite and maghemite phases. The presence of mixture phase was verified by the step-scan X-ray diffraction method. A careful step scan of high angle peaks as (5 1 1) or (4 4 0) revealed distinct magnetite and maghemite peaks and resolved through the deconvolution routine. Their phase quantification was also carried out by constructing a calibration curve using the commercial magnetite and maghemite powders. Accordingly, the iron oxide particles produced by the wire explosion in air contained 55.8 wt.% maghemite and 44.2 wt.% magnetite. In this study, it was well demonstrated that the method can be used as a simple means to differentiate and further quantify the magnetite–maghemite mixture which otherwise requires highly sophisticated equipments and techniques.

Acknowledgments

This research was supported by the Basic Research Project of the Korea Institute of Geoscience and Mineral Resources (KIGAM) funded by the Ministry of Knowledge Economy of Korea.

References

[1] S. Veintemillas-Verdaguer, M.P. Morales, C.J. Serna, Mater. Lett. 35 (1998) 227–231.
[2] G. Schimanke, M. Martin, Solid State Ionics 136–137 (2000) 1235–1240.
[3] S. Veintemillas-Verdaguer, O. Bomatí-Miguel, M.P. Morales, Scr. Mater. 47 (2002) 589–593.
[4] Q. Wang, H. Yang, J. Shi, G. Zou, Mater. Res. Bull. 36 (2001) 503–509.
[5] I. Banerjee, Y.B. Khollam, C. Balasubramanian, R. Pasricha, P.P. Bakare, K.R. Patil, A.K. Das, S.V. Bhoraskar, Scr. Mater. 54 (2006) 1235–1240.
[6] Y.B. Khollam, S.R. Dhage, H.S. Potdar, S.B. Deshpande, P.P. Bakare, S.D. Kulkarni, S.K. Date, Mater. Lett. 56 (2002) 571–577.
[7] F.-Y. Cheng, C.-H. Su, Y.-S. Yang, C.-S. Yeh, C.-Y. Tsai, C.-L. Wu, M.-T. Wu, D.-B. Shieh, Biomaterials 26 (2005) 729–738.

[8] D. Zhang, Z. Tong, S. Li, X. Zhang, A. Ying, Mater. Lett. 62 (2008) 4053–4055.
[9] D. Makovec, A. Košak, A. Žnidaršič, M. Drofenik, J. Magn. Magn. Mater. 289 (2005) 32–35.
[10] G. Visalakshi, G. Venkateswaran, S.K. Kulshreshtha, P.N. Moorthy, Mater. Res. Bull. 28 (1993) 829–836.
[11] C.A. Gorski, M.M. Scherer, Am. Mineral. 95 (2010) 1017–1026.
[12] Y. Qian, Y. Xie, C. He, J. Li, Z. Chen, Mater. Res. Bull. 29 (1994) 953–957.
[13] R. Fan, X.H. Chen, Z. Gui, L. Liu, Z.Y. Chen, Mater. Res. Bull. 36 (2001) 497–502.
[14] K. Woo, J. Hong, S. Choi, H.-W. Lee, J.-P. Ahn, C.S. Kim, S.W. Lee, Chem. Mater. 16 (2004) 2814–2818.
[15] C. Balasubramaniam, Y.B. Khollam, I. Banerjee, P.P. Bakare, S.K. Date, A.K. Das, S.V. Bhoraskar, Mater. Lett. 58 (2004) 3958–3962.
[16] T.J. Daou, G. Pourroy, S. Bégin-Colin, J.M. Grenèche, C. Ulhaq-Bouillet, P. Legaré, P. Bernhardt, C. Leuvrey, G. Rogez, Chem. Mater. 18 (2006) 4399–4404.
[17] A.G. Roca, J.F. Marco, M. d.P. Morales, C.J. Serna, J. Phys. Chem. C 111 (2007) 18577–18584.
[18] J. Wang, M. Yao, G. Xu, P. Cui, J. Zhao, Mater. Chem. Phys. 113 (2009) 6–9.
[19] R. Vijayakumar, Y. Koltypin, I. Felner, A. Gedanken, Mater. Sci. Eng. A 286 (2000) 101–105.
[20] R. Vijaya Kumar, Y. Koltypin, X.N. Xu, Y. Yeshurun, A. Gedanken, I. Felner, J. Appl. Phys. 89 (2001) 6324–6328.
[21] M.M. Can, S. Ozcan, A. Ceylan, T. Firat, Mater. Sci. Eng. B 172 (2010) 72–75.
[22] F. Dubois, C. Mendibide, T. Pagnier, F. Perrard, C. Duret, Corros. Sci. 50 (2008) 3401–3409.
[23] S. Nasrazadani, A. Raman, Corros. Sci. 34 (1993) 1355–1365.
[24] J. Mürbe, A. Rechtenbach, J. Töpfer, Mater. Chem. Phys. 110 (2008) 426–433.
[25] H. Namduri, S. Nasrazadani, Corros. Sci. 50 (2008) 2493–2497.
[26] Y.-H. Zheng, Y. Cheng, F. Bao, Y.-S. Wang, Mater. Res. Bull. 41 (2006) 525–529.
[27] H. Yan, J. Zhang, C. You, Z. Song, B. Yu, Y. Shen, Mater. Chem. Phys. 113 (2009) 46–52.
[28] C.S. Kuivila, J.B. Butt, P.C. Stair, Appl. Surf. Sci. 32 (1988) 99–121.
[29] S.R. Chowdhury, E.K. Yanful, A.R. Pratt, Environ. Earth Sci. 64 (2011) 411–423.
[30] S. Lian, E. Wang, Z. Kang, Y. Bai, L. Gao, M. Jiang, C. Hu, L. Xu, Solid State Commun. 129 (2004) 485–490.
[31] Y.-k. Sun, M. Ma, Y. Zhang, N. Gu, Colloids Surf. A 245 (2004) 15–19.
[32] D. Caruntu, G. Caruntu, Y. Chen, C.J. O'Connor, G. Goloverda, V.L. Kolesnichenko, Chem. Mater. 16 (2004) 5527–5534.
[33] W.W. Yu, J.C. Falkner, C.T. Yavuz, V.L. Colvin, Chem. Commun. (2004) 2306–2307.
[34] K. Simeonidis, S. Mourdikoudis, M. Moulla, I. Tsiaoussis, C. Martinez-Boubeta, M. Angelakeris, C. Dendrinou-Samara, O. Kalogirou, J. Magn. Magn. Mater. 316 (2007) e1–e4.
[35] A. Yan, X. Liu, G. Qiu, N. Zhang, R. Shi, R. Yi, M. Tang, R. Che, Solid State Commun. 144 (2007) 315–318.
[36] A. Yan, X. Liu, G. Qiu, H. Wu, R. Yi, N. Zhang, J. Xu, J. Alloys Compd. 458 (2008) 487–491.
[37] A.C. Doriguetto, N.G. Fernandes, A.I.C. Persiano, E.N. Filho, J.M. Grenèche, J.D. Fabris, Phys. Chem. Miner. 30 (2003) 249–255.
[38] R.E. Vandenberghe, C.A. Barrero, G.M. da Costa, E. Van San, E. De Grave, Hyperfine Interact. 126 (2000) 247–259.
[39] C.A. Gorski, M.M. Scherer, Environ. Sci. Technol. 43 (2009) 3675–3680.
[40] J. Corley, in: P.W. Lee (Ed.), Handbook of Residue Analytical Methods for Agrochemicals, John Wiley & Sons Ltd, Chichester, 2003.